FEDERAL UNIVERSITY OF TECHNOLOGY, AKURE
JOURNAL OF ENGINEERING AND ENGINEERING TECHNOLOGY

INFLUENCE OF BURNING TEMPERATURE ON RICE HUSK ASH MICROSTRUCTURE AND POZZOLANIC REACTIVITY

[1]Omotayo, O.O.*, [1]Omowaye, P.M., [1]Oyerinde, F., [1]Ikumapayi, C.M. and [2]Arum C.
[1]*Department of Civil and Environmental Engineering, Federal University of Technology, Akure, Nigeria*
[2]*Department of Civil and Mining Engineering, JEDS Campus, University of Namibia, Namibia*

**Corresponding author: ooomotayo@futa.edu.ng*

Omotayo O. O., Omowaye P. M., Oyerinde F., Ikumapayi C. M., Arum C. (2026): Influence of Burning Temperature on Rice Husk Ash Microstructure and Pozzolanic Reactivity. FUTA Journal of Engineering and Engineering Technology 20(special), 237-247

Received Date: 15.01.2026 **Accepted Date: 13.03.2026**

Abstract
The excessive CO_2 emissions associated with Portland cement (PC) production have prompted research into sustainable alternatives. Rice husk ash (RHA) is one of the prominent agro-based supplementary cementitious materials that has been used as a sustainable and cost-effective alternative for partially replacing cement in concrete. However, variations in the calcination temperatures have resulted in pronounced differences in the RHA-concrete properties. This study therefore evaluates the effect of the calcination temperature of RHA on the pozzolanic reactivity and microstructural properties of RHA-blended cement concrete. Rice husk samples were obtained in Akure, Nigeria, and were calcined at three specific temperatures, namely, 550°C, 600°C and 650°C. X-ray fluorescence, X-ray diffraction tests, and Scanning Electron Microscopy (SEM) were conducted to evaluate the pozzolanic reactivity and micro-structural properties, respectively, and compressive strength tests were conducted on the RHA-blended cement mixtures. The XRD results showed that all samples of the RHA550 to RHA650 are amorphous based on the peaks shown on the XRD graphs. High silica compounds were also observed (wollastonite, quartz and calcite), which confirm the pozzolanic reactivity of RHA between 550°C and 650°C. The XRF results depicted that the combination of silica (SiO_2), alumina (Al_2O_3) and iron oxide (Fe_2O_3) in each sample is more than 70% in accordance with ASTM. The results of the setting time tests indicated that the addition of RHA accelerated the setting time from 567 mins for the control mix to 442 mins for the RHA650 mix. Compressive strength results showed that RHA600 performed best in terms of pozzolanic reactivity and strength, recording a strength of 18.2 N/mm² compared to 15.7 N/mm² for the control specimen at 56 days of curing. It is thus preferred for obtaining optimal concrete results. This research provides a validation for the adoption and processing of RHA for commercial use in the construction industry.

Keywords: *Pozzolanic Reactivity, Rice Husk Ash, Burning Temperature, Supplementary Cementitious Materials, Sustainable Concrete.*

Introduction

One of the major problems discussed across the globe is the excess emission of CO_2 to the environment. The construction industry has been recognized to contribute significantly to this problem through the production of the Portland cement (PC), which constitutes about 5-7% of total annual greenhouse emissions (Miller *et al*., 2021). These emissions are projected to reach 1.4 - 3.8 Gt by 2050 in comparison with an annual emission of 0.7 Gt as of the year 2018 (Cheng *et al*., 2023). Furthermore, the heightened cost of cement in recent times due to inflation makes cement highly expensive for construction.

These reasons, among others, have necessitated the search for suitable alternatives that can partially replace Portland cement in concrete production. These materials, usually of natural, industrial or agro-based origins, also known as supplementary cementitious materials (SCMs) or pozzolans,

generally do not possess cementitious properties on their own, but in finely ground form and in the presence of water and calcium hydroxide, they can react to form cementitious compounds (Becerra-Duitama & Rojas-Avellanda, 2022). They have been found not only to improve cementitious properties but also to improve other properties of concrete, including mechanical, durability, and rheological properties (Alabi & Mahachi, 2022; Arum *et al*., 2022; Ikumapayi *et al*., 2021; Pradhan *et al*., 2024). Examples of natural pozzolans include volcanic ashes, diatomaceous earth, and pumite, while fly ash, slag, silica fume are generally referred to as industrial pozzolans (Ayub *et al*., 2021). These pozzolan types are sometimes difficult to obtain, especially in areas with low level of industrial activities. Agro-based pozzolans (such as rice husk ash, palm oil fuel ash, coconut husk ash), however, are more widely available and easier to procure and process than the industrial ones (Alsubari *et al.*, 2022). This makes them highly valuable for construction, especially in developing countries.

Many researchers have discovered promising results from studies on the use of agro-based pozzolans in concrete. For instance, Ikumapayi *et al*. (2021) evaluated the hydration efficiency and reactivity of groundnut shell ash (GSA) in concrete. The study showed that at an optimal 8% GSA addition, the integrity of the microstructural interlock and hydration behaviour of concrete is improved. A study by Akeke *et al*. (2023) indicated that palm oil fuel ash (POFA) showed satisfactory strength performance at 35% addition in concrete. Lejano *et al.* (2024) investigated the mechanical strength performance of coconut shell granules (CSG) and coconut shell ash (CSA) in coconut coir (CC) reinforced concrete. The results showed that a combination of CSG and CCA in 2% CC reinforced concrete proved viable for low-strength concrete production. Al-Alwan *et al*. (2024) studied the impact of RHA on concrete strength and durability properties and observed that the addition of fine RHA particles to concrete resulted in improved compressive, flexural, and tensile strength and inhibition of chloride ion penetration with time.

Despite this wide range of results on the effectiveness of these pozzolans in concrete, one of the limitations to their adoption has been the lack of standardization in the processing of the pozzolans for optimal results. It has been observed that there are usually variations in the strength and durability performance of pozzolanic concrete produced when the pozzolans are calcinated at different temperatures. These variations have also been found to be sometimes significant. For instance, Faried *et al*. (2021) observed that production of nano rice husk ash (NRHA) at different temperatures for use in ultra-high-performance concrete resulted in varying results at different burning temperatures, with the optimum results achieved when NRHA was burnt at 700℃ for 5 hours. The impact of RHA on the activity and performance of concrete with calcination of RHA at 650℃, 800℃ and 900℃ was investigated by Tian *et al*. (2021). Best durability performance, including carbonization resistance and frost resistance, was achieved at 650℃ burning temperature. This uncertainty in performance prevents reliability in the results obtainable from pozzolan use in concrete. In a bid to address this problem, this research sought to investigate the effects of calcination temperatures on the pozzolanic reactivity and microstructural properties of rice husk ash (RHA) blended cement. The choice of RHA was due to its wide availability and consistently promising performance it shows when used in concrete. The scope of the research was limited to evaluating the pozzolanic reactivity, microstructural properties, and strength properties of the RHA-blended cement concrete.

Materials and Methods

Collection and Preparation of Materials

A substantial amount of rice husks was obtained from local sources and transported to a kiln located at the Department of Industrial Design (IDD), Federal University of Technology, Akure, for calcination. The rice husks were loaded into the kiln and fired using gas nozzles to the required temperatures, including 550℃, 600℃, and 650℃ with a holding-down time of 2 hours. The temperature readings were taken using a thermocouple thermometer attached to a long pin and inserted into the kiln through a small drilled hole behind the kiln. The rice husk ash obtained at each of the different burning temperatures was sieved into fine particles and mixed with cement at 10% replacement. The choice of this dosage rate is based

on prior literature and experimental studies (Endale *et al*., 2022; Liu *et al*., 2024; Nduka *et al*., 2022; Valenzuela *et al*., 2025). Water was then added to this mixture to form a paste, which was filled into small-sized cylindrical molds 30 mm in diameter and allowed to set for 24 hours before being demolded. The test specimens were cured under water for 7 and 28 days. At each curing age, the RHA-OPC specimens were removed from the water, air-dried, and pulverized into fine particles. These crushed test samples were then subjected to XRD, XRF, and SEM analysis to investigate their crystal structure and phase composition, mineralogical compositions, and microstructural properties, respectively.

X-ray Fluorescence test

The surface on which the sample was to be analyzed was cleaned to remove any surface contamination that could affect the accuracy of the test. The XRF instrument was calibrated using certified reference materials with known elemental composition. This ensured that the instrument was accurately measuring the elemental composition of each sample. The sample was placed in the XRF instrument, and a beam of X-rays was directed onto the sample. The X-rays excited the electrons in the sample, causing them to emit characteristic fluorescent X-rays. The energies and intensities of the emitted X-rays were measured by the XRF detector, which generated a spectrum showing the intensity of the X-rays emitted by each element in the spectrum. This spectrum was then compared with a database of known X-ray spectra to identify the elements present in the sample and their respective concentrations.

X-ray Diffraction Test

The sample to be analyzed was placed on a flat surface, typically a glass slide or a silicon wafer. A beam of X-rays generated from a calibrated XRD instrument was directed to the sample. This caused diffraction patterns to be produced. A detector was used to collect diffraction patterns, and the results were recorded as a series of peaks. The diffraction peaks were analyzed to determine the crystal structure and phase composition of the sample. The results of the XRD analysis were reported as a list of the identified crystal structures and phases present in the sample.

Scanning Electron Microscopy (SEM)

Using a scanning electron microscope, the microstructural properties of the RHA-OPC cement paste was investigated, in order to study the impact of the calcination temperature on the shape, morphology, structure, and mechanical properties of the matrix. The microscope settings were adjusted based on the specific analysis requirements. Subsequently, the electron beam was scanned across the sample surface, and the emitted secondary electrons were detected to create an image of the sample. The obtained images and data were analyzed and interpreted to draw inferences about the structure, composition, and properties of the sample.

Compressive Strength Test

Separate concrete mixtures containing a combination of RHA (at each burning temperature), OPC, fine aggregates, coarse aggregates, and water, using a 1:2:4 mix ratio, were prepared and cast into steel moulds sized 150 mm3150 mm3150 mm. These samples were prepared to investigate the compressive strength of the concrete produced using the RHA samples calcinated at the specified temperatures. These samples were cured for 7, 28 and 56 days. The cured samples were subjected to compressive strength tests under a Universal Testing Machine, and the strengths at failure were recorded. These values were analyzed and plotted on a graph.

Results and Discussion

Characterization of RHA Silica Structure

In the X-ray diffraction results for rice husk ash (RHA) calcined at 550°C, 600°C and 650°C, the observed peaks for the rice husk ash (RHA) calcined at different temperatures showed the presence of quartz (silicon dioxide), illite (hydrated potassium aluminum silicate), muscovite (potassium aluminum silicate), chlorite, and orthoclase (potassium aluminum silicate). These different silicate minerals all have different compositions that affect the pozzolanic reactivity of RHA with blended cement. The X-ray diffraction test for the

RHA samples at different temperatures are presented in Figures 1 to 3, respectively. In a general RHA X-ray spectrum, a broad amorphous peak is typically present (Samuel *et al*., 2023). However, if the RHA possesses a crystalline nature, it will manifest as a distinct peak atop the prominent amorphous peak. In the case of the RHA550 and RHA600 samples, broad peaks were observed as shown in Figures 1 and 2, primarily indicating the amorphous nature of the samples. RHA650 also exhibits an amorphous structure based on the broad peaks shown in Figure 3. Although some traces of crystallinity are noticed, they could be considered less significant, due to their low intensities relative to other portions of the sample.

The pie chart in Figure 1 represents the noticeable compounds observed in the RHA550 sample, which suggests the active presence of quartz (44% - ICDD 00-002-0471), muscovite (34% - ICDD 00-002-0467) and orthoclase (10% - ICDD 00-002-0475) as the major minerals. From the pie charts in Figures 2 and 3, RHA600 sample showed the presence of quartz (36% - ICDD 00-002-0471), muscovite (31% - ICDD 00-002-0467) and illite (15% - 00-002-0050) while the RHA650 sample exhibited the predominance of quartz (46%), orthoclase (30.3%) and muscovite (18.3%) respectively.

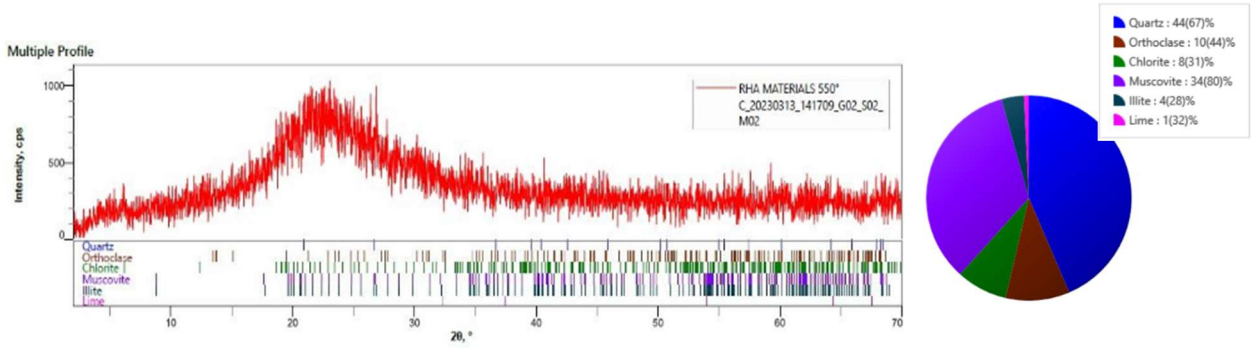

Figure 1. X-ray Diffraction results showing predominant minerals in the RHA sample calcined at 550ºC

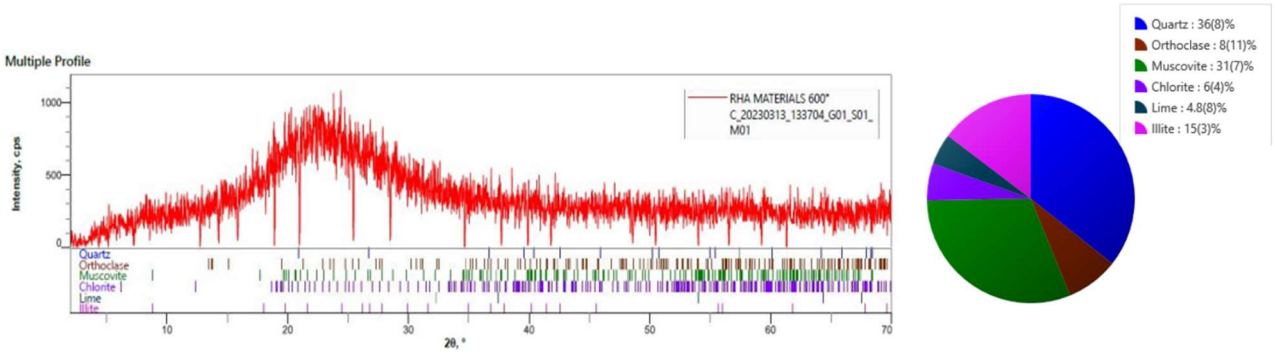

Figure 2. X-ray Diffraction results showing predominant minerals in the RHA sample calcined at 600ºC

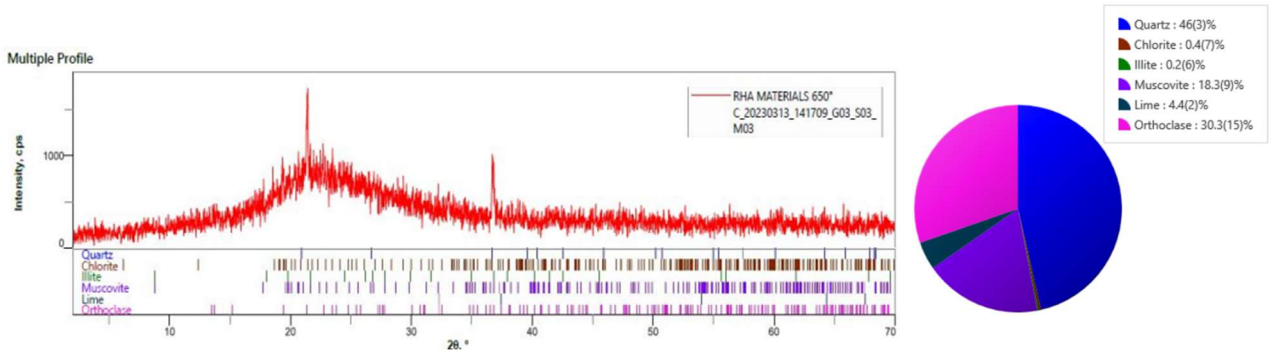

Figure. 3. X-ray Diffraction results showing predominant minerals in the RHA sample calcined at 650°C

When the RHA samples were blended with cement at 10% dosage rate, the XRD patterns showed the predominance of wollastonite (52%), calcite (18.4%), and quartz (13%) for RHA550+OPC, calcite (61%), quartz (14.3%), and albite (11%) for the RHA600+OPC sample, and calcite (57%), orthoclase (29%), and quartz (9.1%) for the RHA650+OPC sample respectively. These can be seen in Figures 4 to 6. The XRD structures for the three blended RHA+OPC samples showed a predominantly amorphous pattern with slight indications of crystallinity.

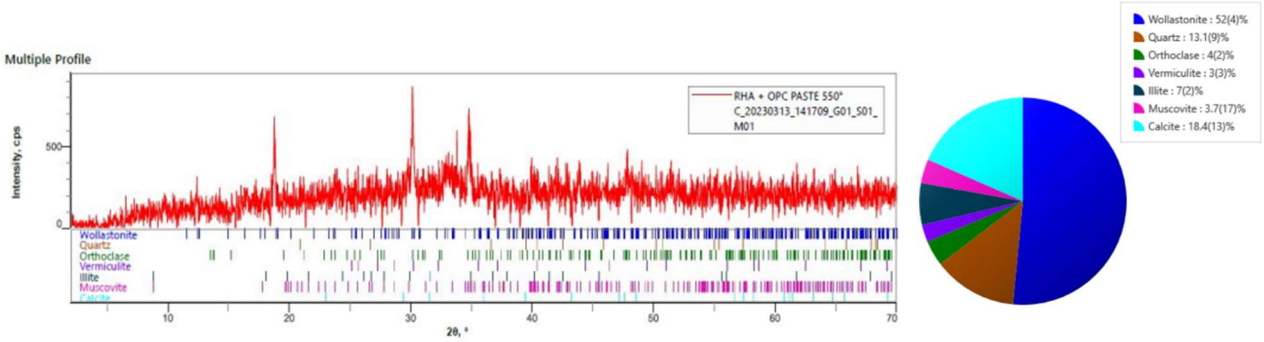

Figure. 4. X-ray Diffraction results showing predominant minerals in the RHA sample calcined at 550°C mixed with blended cement (7 days)

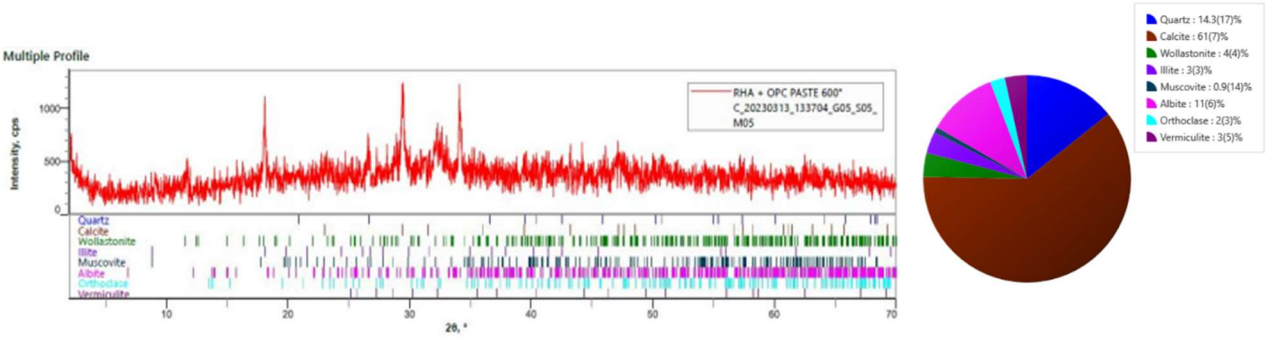

Figure 5. X-ray Diffraction results showing predominant minerals in the RHA sample calcined at 600oC mixed with blended cement (7 days)

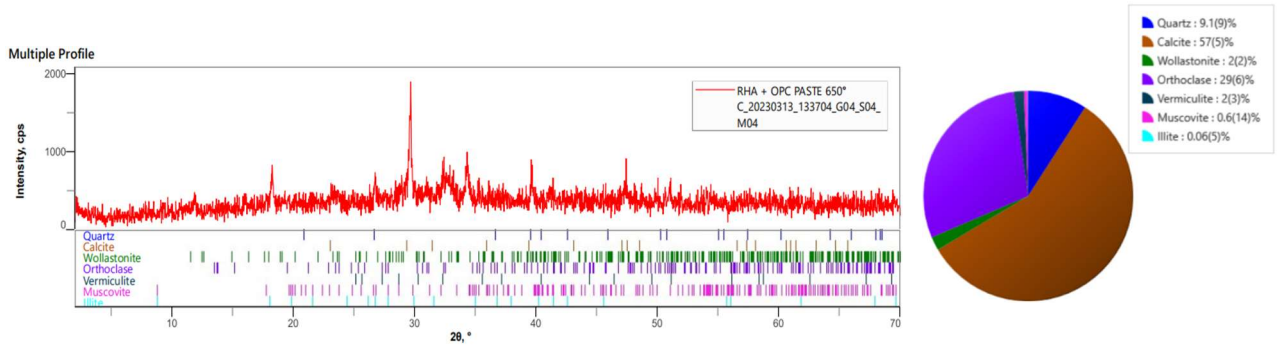

Figure 6. X-ray Diffraction results showing predominant minerals in the RHA sample calcined at 650oC mixed with blended cement (7 days)

Chemical Oxide Compositions of RHA

The results of the XRF tests to determine the oxide compositions of the RHA samples are presented in Table 1. The results showed that RHA550 possessed 72.19% silica content, RHA600 had 71.68%, and RHA650 had the highest amount of silica content (73.47%). Altogether, the combination of silica (SiO_2), alumina (Al_2O_3), and ferric oxide (Fe_2O_3) for all the RHA samples exceeded 70%, and the SO_3 content was less than 5%. They can thus be classified as Class-N pozzolans according to ASTM C618-12a (2012). Meanwhile, the Al_2O_3 content was least for RHA600 at 0.9%, while RHA550 had 1.557% and RHA600 had 1.717% alumina content. Vyšvařil *et al*. (2024) showed that the presence of appropriate alumina content is essential to the formation of calcium-aluminate-hydrate (CAH), which is very instrumental to concrete strength development. The Fe_2O_3 contents for the RHA samples fairly ranged between 1.4% and 2.034%. Studies by Ghorbel & Samet (2013) and Largeau *et al*. (2018) show that Fe_2O_3 has a positive effect on concrete compressive strength, especially when in amounts less than 2.5 - 2.7%. It was further observed that all three RHA samples contained high level of phosphorus pentoxide (P_2O_5). Xie *et al.* (2021) explained that high content of phosphorus will reduce the content of C_3S and make the formation of C_2S and C_3P, whose hydration reactivity is rather lower, such that on one hand less hydrated products, such as calcium silicate hydrate (C-S-H) gel, can be obtained, and on the other hand, the hydration reaction will be slowed by severely prolonging the induction period that calcium oxide (CaO) reacts with water to form calcium hydroxide ($Ca(OH)_2$) during the early stages of cement hydration. This reaction contributes to the overall hydration process of cement, leading to the formation of calcium silicate hydrates (C-S-H) gel. C-S-H gel is the primary binder in concrete, providing strength and stability. The percentage of CaO content was relatively similar with the three RHA samples with RHA550 having the highest percentage (2.97%).

Table 1: Chemical Composition of RHA Samples based on X-ray Fluorescence test results

Chemical Composition (% wt. of ash)	**RHA Samples RHA550**	**RHA600**	**RHA650**
SiO_2	72.192	71.68	73.467
V_2O_5	0.013	0.012	0.001
Cr_2O_3	0.01	0.01	0.008
MnO	0.332	0.332	0.271
Fe_2O_3	2.034	1.553	1.403
NiO	0.003	0.001	0.001
CuO	0.068	0.063	0.054
Nb_2O_3	0.011	0.011	0.009

P_2O_5	12.179	14.329	12.889
SO_3	1.029	0.74	0.651
CaO	2.967	2.654	2.638
MgO	0.24	0	0.332
K2O	5.994	6.247	5.406
Al_2O_3	1.557	0.9	1.717
Ta_2O_5	0.016	0.025	0.014
TiO_2	0.192	0.24	0.171
ZnO	0.115	0.109	0.083
Ag_2O	0.014	0.007	0.013
Cl	0.947	1	0.791

Microstructure of RHA Samples Mixed with Ordinary Portland cement

The examination of the microstructural properties of the RHA-OPC samples helped to study the shape, size and morphological characteristics of the paste in terms of the RHA calcination temperature and the strength properties of the matrix. The scanning electron micrographic (SEM) observations of the RHA+OPC samples cured for 7 days, at a magnification of 8000X and a resolution of 100µm, are presented in Figures 7 – 12.

Figures 7 and 8 represent the SEM image and elemental composition of the RHA550+OPC respectively. It can be observed that the sample exhibited a dominant fibrous/acicular calcium-silicate-hydrate (C-S-H) network with interconnected porosity, forming a dense interwoven matrix indicative of good strength properties. The EDX composition having a high Ca/Si ratio, approximately 1.5, suggests well-formed C-S-H and successful pozzolanic reaction. This explains the reason behind the RHA550+OPC sample exhibiting the highest strength at 7 days of curing. Feng *et al*. (2013) in allusion to this highlighted that the average Ca/Si ratio is 1.75, and facilitates development of C-S-H bonds. The high concentrations of oxygen (40.2%) and calcium (15.65%) further confirm the predominant presence of hydrated calcium-based phases, especially C-S-H, which is rich in calcium and oxygen. The notable presence of aluminum (3.2%) also shows an active participation of the RHA550 pozzolan in the hydration reaction, resulting in the formation of calcium aluminate silicate hydrate (C-A-S-H).

Figures 9 and 10 show the SEM image and elemental composition of the RHA600+OPC sample. In contrast to the RHA550+OPC sample, this sample shows a more granular and particulate morphology with significantly less prominent fibrous C-S-H. The EDX analysis indicates higher proportions of Ca and Si, suggesting a larger fraction of unreacted cement clinker and pozzolan particles, or less formation of binding C-S-H. The pore structure shows a higher degree of inter-particulate porosity compared to the fibrous C-S-H rich microstructure of RHA550+OPC. The higher Ca/Si ratio (approximately 1.98) suggests a less mature C-S-H or a lower degree of pozzolanic reaction. The

presence of higher calcium content (40.2%) and lower oxygen content (20.2%) compared with the previous sample further confirms a higher proportion of calcium-rich, unhydrated or less-hydrated phases, such as calcium silicates (C_3S or C_2S) or unreacted calcium hydroxide (CH). Endale *et al.* (2022) and Xu *et al.* (2012) also alluded to the porous and non-uniform nature of RHA particles.

The SEM image and elemental composition of the RHA650+OPC sample are presented in Figures 11 and 12 respectively. This sample shows a distinct microstructure compared to the earlier described ones, showing the dominance of abundant needle-like ettringite crystals. Even though ettringite is a normal hydration product, its volume as shown in the image suggests possibly conditions that favour its formation over a dense C-S-H matrix. The exceptionally high Ca/Si ratio (approximately 6.84) confirms the prevalence of the calcium-rich non-C-S-H binding phases (like ettringite, calcium hydroxide or calcium carbonate). It can be implied that the higher calcination temperature significantly altered the hydration chemistry, promoting the formation of voluminous ettringite at the expense of a denser C-S-H network, hence reducing the overall pozzolanic efficiency. This sample also exhibited the highest carbon content and very high calcium, strongly indicating a greater degree of calcium-carbonate presence. Thus, the more porous and less stable microstructure observed with this sample, and other observations made can be attributed to its low early strength gain compared to the other two samples.

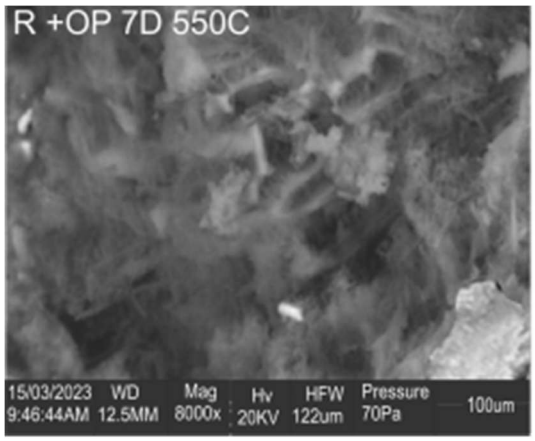

Figure 7. SEM image RHA 550 + OPC after 7 curing days

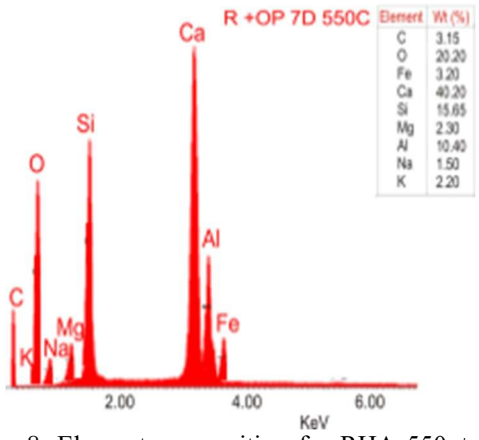

Figure 8. Element composition for RHA 550 + OPC after 7 curing days using EDX

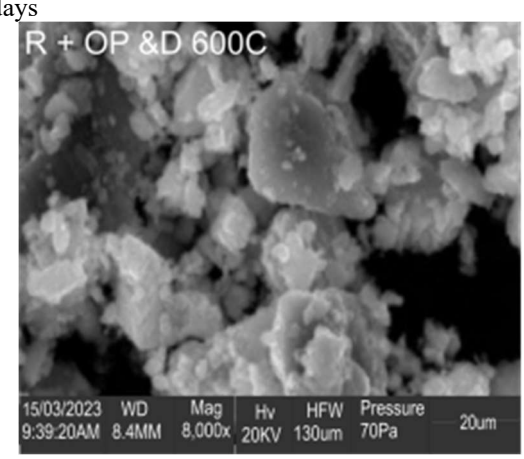

Figure 9. SEM image RHA 600 + OPC after 7 curing days

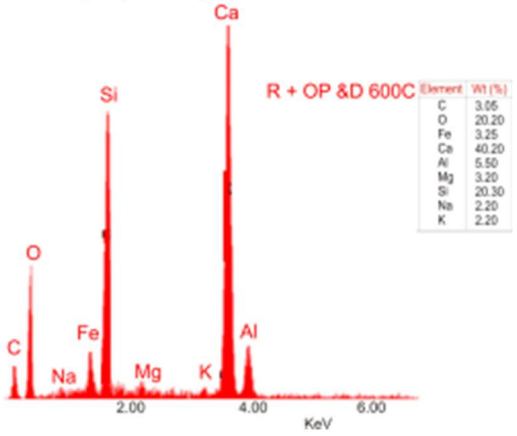

Figure 10. SEM image RHA 550 + OPC after 7 curing days

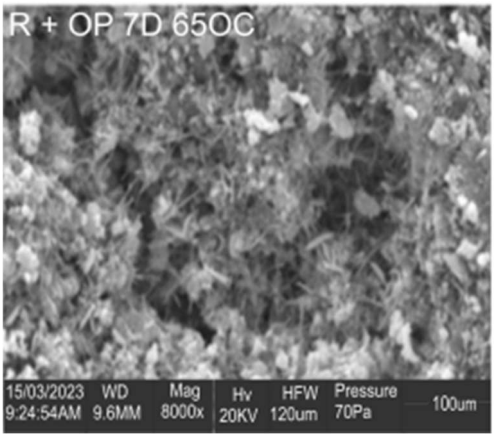

Figure 11. SEM image RHA 650 + OPC after 7 curing days

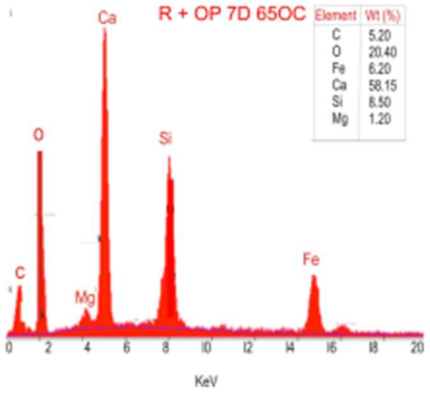

Figure 12. Element composition for RHA 650 + OPC after 7 curing days using EDX

Setting Time of RHA-OPC Concrete

Setting time test results for the RHA-OPC concrete samples are presented in Figure 13. It can be seen from the results that both initial and final setting times of the concrete decreased with the burning temperature at which the RHA was calcined. RHA650 had the least final setting time at 442 mins, which was 22% lower than the final setting time of the control concrete. This trend can be attributed to

the high amorphous content of the RHA particles and increased water demand with increasing temperature, which may have resulted in faster initial consumption of $Ca(OH)_2$ released from the cement hydration. Chanu & Devi (2013) observed a similar trend noting that RHA unlike other pozzolans, tend to reduce the final setting time of cement.

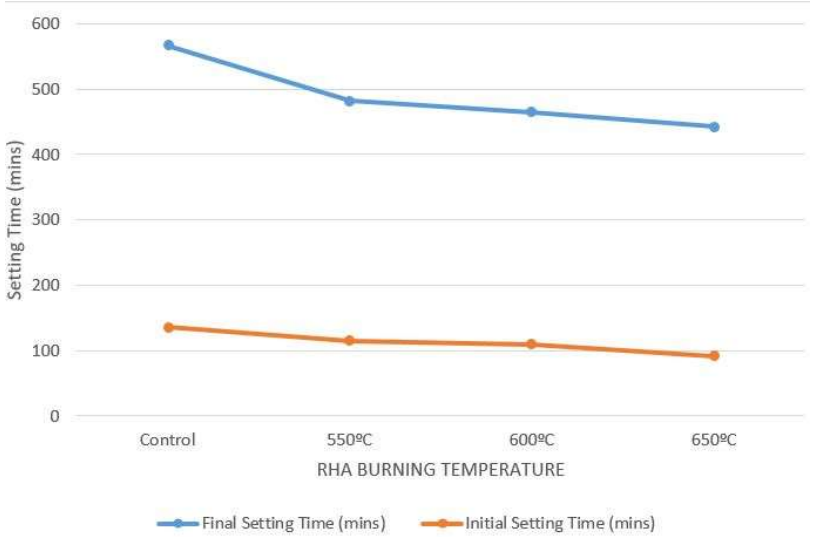

Figure 13. Setting-Time Test Chart for Varied Temperature of RHA

Compressive Strength of RHA Mixed with Ordinary Portland cement (OPC) At Different Curing Ages with Mix Ratio 1:2:4

The average compressive strength of partially replaced cement with 10% of rice husk ash (RHA550 + OPC, RHA600 + OPC, RHA650 + OPC) concrete specimen is shown in Figure 14. At early ages, RHA550 showed the highest compressive strength, which may be due to high SiO_2 content shown in Table 1. Studies by Nair *et al.* (2008) and Zahedi *et al*. (2015) have shown that incineration temperature is a major contributor to the quality of silica produced, and that high amorphous silica contributes significantly to early-age strength of concrete. RHA650 showed the least compressive strength (10.48 N/mm^2) compared to the other samples. It should also be noted that RHA650 had a higher w/c (water to cement ratio) during concrete production. The RHA650 elemental composition in Figure 12 shows that RHA650 had the highest calcium percentage weight compared to other samples. This suggests that the pozzolanic reaction might be occurring faster at this temperature, consuming and reducing the calcium hydroxide available for the initial cement hydration, hence its shorter setting time and low early strength compared to other samples. Yeshiwas *et al*. (2025), Amin *et al.* (2019), and Raheem & Kareem (2017) also observed similar trends with RHA in partial replacement of concrete.

RHA650 initially showed stronger compressive strength performance at 28 days (23.18 N/mm^2), but a later decline at 56 days. Although, RHA550 registered the least compressive strength at 28 days (13.95 N/mm^2), it outperformed the strength of the control concrete after 56 days of curing. All samples of RHA showed comparatively better performance than the control concrete at 56 days, indicating the long-term pozzolanic activity and strength gain associated with pozzolans in concrete. RHA600 showed the most consistent performance with a continuous strength gain from 12.72 N/mm^2 to 18.16 N/mm^2. It also had the highest compressive strength after 56 days of curing. This suggests that RHA calcined at 600^{o}C is more balanced and effective in terms of pozzolanic activity and performance compared to other burning temperatures when added at an optimal dosage rate of 10%. Similar results and observations were made by Nduka *et al.* (2022), Endale *et al*. (2022), and Agboola *et al*. (2022).

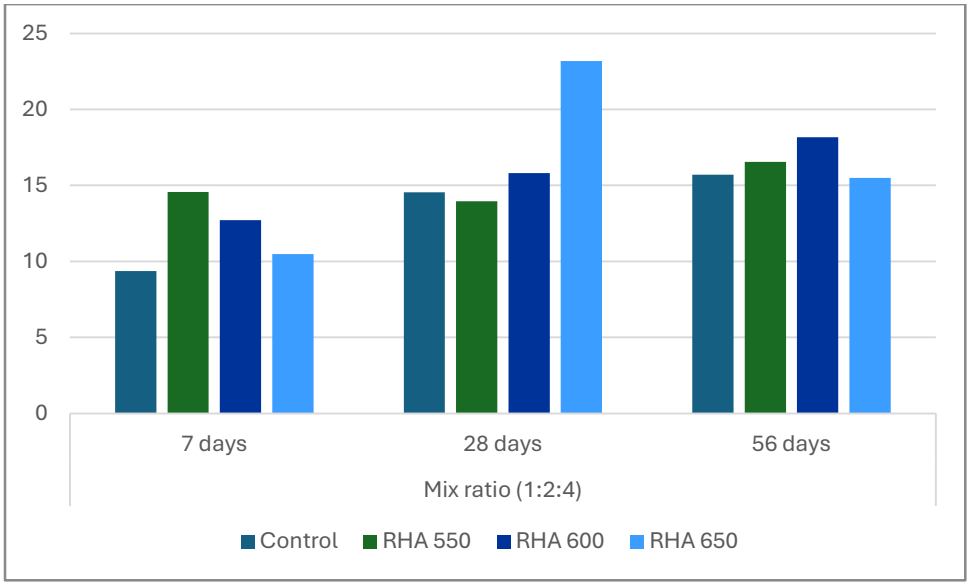

Figure 14. Variation of Compressive strength of the RHA concrete samples at different curing ages

Conclusion

In conclusion, the investigation of the pozzolanic reactivity and micro-structural properties of rice husk ash (RHA) produced at different burning temperatures and combined with blended cement is an effort to improve their adoptability in the construction industry. The research showed that incorporating a 10% partial replacement of cement in concrete, subjected to burning temperatures of 550°C, 600°C, and 650°C, yields satisfactory and desired outcomes comparable to the control group.

Based on a comprehensive analysis of the experimental results, the following conclusions can be drawn:

- The presence of high silica compounds and amorphous materials in rice husk ash contributed to the formation of additional calcium silicate hydrates (C-S-H) gel, enhancing the strength and durability properties of the blended cement.
- The incorporation of RHA in blended cement influenced the microstructure of the cementitious matrix. The presence of voids and pores led to improved mechanical properties and reduced permeability of the blended cement
- Rice husk ash calcined at 550ºC, 600ºC and 650ºC mixed with blended cement produced a higher compressive strength than the control, with the optimum strength attained at RHA calcination at 600ºC.
- The setting time of rice husk ash blended cement concrete falls within the standard range, eliminating the need for admixtures except for special conditions.
- Hydration of the concrete is affected by the temperature at which the rice husk is calcined, as the temperature increases and demands more water and this is due to the content of Calcium oxide presence in the Rice husk ash.

Recommendation

It is recommended that RHA is calcined to 600°C at a 10% replacement of cement in order to achieve optimal compressive strength. Further studies can be channeled towards evaluating durability and rheological properties of RHA-based pozzolanic concrete for other applications such as 3D-printability.

Acknowledgement

The authors appreciate the Tertiary Education Trust Fund (TETFund) in Nigeria for partially funding this research from Institution Based Research Fund (IBRF) 2018-2019 with reference number VCPU/TETFund/155C. The authors also acknowledge Engr. S. P. Akande and the Department of Civil and Environmental Engineering, the Federal University of Technology Akure for the laboratory support during the research.

References

Agboola, S. A., Yunusa, U., Tukur, M., & Bappah, H. (2022). Strength Performance of Concrete Produced with Rice Husk Ash as Partial Replacement of Cement. *African Journal of Environmental Sciences and Renewable Energy*, *5*(1), Article 1.

Akeke, G. A., Inem, P. E. U., Alaneme, G. U., & Nyah, E. E. (2023). Experimental investigation and modelling of the mechanical properties of palm oil fuel ash concrete using Scheffe's method. *Scientific Reports*, *13*(1), 18583. https://doi.org/10.1038/s41598-023-45987-3

Alabi, S. A., & Mahachi, J. (2022). Performance assessment of mechanical and durability properties of cupola slag geopolymer concrete with fly and rice husk ashes. *Nigerian Journal of Technological Development*, *19*(1), 27–38.

Al-Alwan, A. A. K., Al-Bazoon, M., Mussa, F. I., Alalwan, H. A., Shadhar, M. H., Mohammed, M. M., & Mohammed, M. F. (2024). The impact of using rice husk ash as a replacement material in concrete: An experimental study. *Journal of King Saud University-Engineering Sciences*, *36*(4), 249–255.

Alsubari, B., Shafigh, P., Jumaat, M. Z., Ghayeb, H. H., & Alqawzai, S. (2022). Self-compacting concrete containing high volume palm oil fuel ash: Cost, sustainability, and applications. *International Journal of Sustainable Building Technology and Urban Development*, *13*(2), 148–154.

Amin, M. N., Hissan, S., Shahzada, K., Khan, K., & Bibi, T. (2019). Pozzolanic Reactivity and the Influence of Rice Husk Ash on Early-Age Autogenous Shrinkage of Concrete. *Frontiers in Materials*, *6*. https://doi.org/10.3389/fmats.2019.00150

Arum, R. C., Arum, C., & Alabi, S. A. (2022). The highs and lows of incorporating pozzolans into concrete and mortar: A review on strength and durability. *Nigerian Journal of Technology*, *41*(2), 197–211.

ASTM C618-12a. (2012). *Standard Specification for Coal Fly Ash and Raw or Calcined Natural Pozzolan for Use in Concrete*. American Society of Testing and Materials (ASTM International), West Conshohocken, PA, USA.

Ayub, M., Othman, M. H. D., Khan, I. U., Hubadillah, S. K., Kurniawan, T. A., Ismail, A. F., Rahman, M. A., & Jaafar, J. (2021). Promoting sustainable cleaner production paradigms in palm oil fuel ash as an eco-friendly cementitious material: A critical analysis. *Journal of Cleaner Production*, *295*, 126296. https://doi.org/10.1016/j.jclepro.2021.126296

Becerra-Duitama, J. A., & Rojas-Avellanda, D. (2022). Pozzolans: A review. *Engineering and Applied Science Research (EASR)*, *49*(4), 495–504.

Chanu, N. M., & Devi, D. T. K. (2013). Contribution Of Rice Husk Ash To The Properties Of Cement Mortar And Concrete. *International Journal of Engineering Research*, *2*(2).

Cheng, D., Reiner, D. M., Yang, F., Cui, C., Meng, J., Shan, Y., Liu, Y., Tao, S., & Guan, D. (2023). Projecting future carbon emissions from cement production in developing countries. *Nature Communications*, *14*(1), Article 1. https://doi.org/10.1038/s41467-023-43660-x

Endale, S. A., Taffese, W. Z., Vo, D.-H., & Yehualaw, M. D. (2022). Rice husk ash in concrete. *Sustainability*, *15*(1), 137.

Faried, A. S., Mostafa, S. A., Tayeh, B. A., & Tawfik, T. A. (2021). The effect of using nano rice husk ash of different burning degrees on ultra-high-performance concrete properties. *Construction and Building Materials*, *290*, 123279.

Feng, D., Xie, N., Gong, C., Leng, Z., Xiao, H., Li, H., & Shi, X. (2013). Portland cement paste modified by TiO2 nanoparticles: A microstructure perspective. *Industrial & Engineering Chemistry Research*, *52*(33), 11575–11582.

Ghorbel, H., & Samet, B. (2013). Effect of iron on pozzolanic activity of kaolin. *Construction and Building Materials*, *44*, 185–191.

https://doi.org/10.1016/j.conbuildmat.2013.02.068

Ikumapayi, C. M., Arum, C., & Alaneme, K. K. (2021). Reactivity and hydration behavior in groundnut shell ash based pozzolanic concrete. *Materials Today: Proceedings*, *38*, 508–513.

Largeau, M. A., Mutuku, R., & Thuo, J. (2018). Effect of Iron Powder (Fe2O3) on Strength, Workability, and Porosity of the Binary Blended Concrete. *Open Journal of Civil Engineering*, *8*(4), Article 4. https://doi.org/10.4236/ojce.2018.84029

Lejano, B., Elevado, K. J., Fandiño, M. A., Ng, E. A., Datinguinoo, Z. A. N., & Oliveros, S. B. (2024). Experimental investigation of utilizing coconut shell ash and coconut shell granules as aggregates in coconut coir reinforced concrete. *Cleaner Engineering and Technology*, *21*, 100779.

Liu, B., Wang, S., Jia, W., Ying, H., Lu, Z., & Hong, Z. (2024). The Effect of RHA as a Supplementary Cementitious Material on the Performance of PCM Aggregate Concrete. *Buildings*, *14*(7), Article 7. https://doi.org/10.3390/buildings14072150

Miller, S. A., Habert, G., Myers, R. J., & Harvey, J. T. (2021). Achieving net zero greenhouse gas emissions in the cement industry via value chain mitigation strategies. *One Earth*, *4*(10), 1398–1411. https://doi.org/10.1016/j.oneear.2021.09.011

Nair, D. G., Fraaij, A., Klaassen, A. A. K., & Kentgens, A. P. M. (2008). A structural investigation relating to the pozzolanic activity of rice husk ashes. *Cement and Concrete Research*, *38*(6), 861–869. https://doi.org/10.1016/j.cemconres.2007.10.004

Nduka, D. O., Olawuyi, B. J., Fagbenle, E. O., & Fonteboa, B. G. (2022). Mechanical and microstructural properties of high-performance concrete made with rice husk ash internally cured with superabsorbent polymers. *Heliyon*, *8*(9), e10502. https://doi.org/10.1016/j.heliyon.2022.e10502

Pradhan, S. S., Mishra, U., Biswal, S. K., Pramanik, S., Jangra, P., & Aslani, F. (2024). Effects of rice husk ash on strength and durability performance of slag-based alkali-activated concrete. *Structural Concrete*, *25*(4), 2839–2854. https://doi.org/10.1002/suco.202300173

Raheem, A. A., & Kareem, M. (2017). Chemical Composition and Physical Characteristics of Rice Husk Ash Blended Cement. *International Journal of Engineering Research in Africa*, *32*, 25–35. https://doi.org/10.4028/www.scientific.net/JERA.32.25

Samuel, G. A., Adele, G., & Ali, E. (2023). *Microstructure and Shrinkage Behaviour of Glass Ceramics Developed from Synthesis of Rice Husk Ash as a Source of Silica*. *Maiden Edition*, 17–27.

Tian, E., Frank Chen, Y., Zhuang, Y., & Zeng, W. (2021). Effects of rice husk ash on itself activity and concrete behavior at different preparation temperatures. *Materials Testing*, *63*(11), 1070–1076.

Valenzuela, M., Tuninetti, V., Ciudad, G., Miranda, A., & Oñate, A. (2025). Designing sustainable cement free compositions with rice husk ash to improve mechanical performance in next generation ecoblocks. *Scientific Reports*, *15*(1), 14920. https://doi.org/10.1038/s41598-025-97963-8

Vyšvařil, M., Žižlavský, T., Dvořák, K., & Spychał, E. (2024). Long-term mechanical properties of lime-pozzolan mortars: The role of amorphous Al_2O_3. *MATEC Web of Conferences*, *403*, 02009. https://doi.org/10.1051/matecconf/202440302009

Xie, L., Deng, M., Tang, J., & Liu, K. (2021). Hydration and Strength Development of Cementitious Materials Prepared with Phosphorous-Bearing Clinkers. *Materials*, *14*(3). https://doi.org/10.3390/ma14030508

Xu, W., Lo, T., & Memon, S. (2012). Microstructure and reactivity of rich husk ash. *Construction and Building Materials*, *29*, 541–547.

https://doi.org/10.1016/j.conbuildmat.2011.11.005

Yeshiwas, M. D., Yehualaw, M. D., Habtegebreal, B. T., Nebiyu, W. M., & Taffese, W. Z. (2025). Rice Husk Ash and Waste Marble Powder as Alternative Materials for Cement. *Infrastructures*, *10*(4), Article 4. https://doi.org/10.3390/infrastructures10040078

Zahedi, M., Ramezanianpour, A. A., & Ramezanianpour, A. M. (2015). Evaluation of the mechanical properties and durability of cement mortars containing nanosilica and rice husk ash under chloride ion penetration. *Construction and Building Materials*, *78*, 354–361. https://doi.org/10.1016/j.conbuildmat.2015.01.045